First-principles study of the rectifying properties of Pt/TiO_2 interface

Tomoyuki Tamura,[1,2] Shoji Ishibashi,[1,2] Kiyoyuki Terakura,[1,3,2] and Hongming Weng[3,2]
[1]*Research Institute for Computational Sciences (RICS), National Institute of Advanced Industrial Science and Technology (AIST), 1-1-1 Umezono, Tsukuba, Ibaraki 305-8568, Japan*
[2]*JST, CREST, Kawaguchi, Saitama 332-0012, Japan*
[3]*Research Center for Integrated Science (RCIS), Japan Advanced Institute of Science and Technology (JAIST), 1-1 Asahidai, Nomi, Ishikawa 923-1292, Japan*

(Received 5 June 2009; revised manuscript received 5 October 2009; published 3 November 2009)

First-principles calculations have been performed to study the interface electronic structure of Pt/TiO_2 and to analyze the rectifying property of the Pt/TiO_2/Pt structure. For the stoichiometric interface, the metal-induced gap states (MIGS) have amplitude appreciably only at the interface TiO_2. We will show that the presence of MIGS makes oxygen-vacancy formation energy small at the interface. It is therefore expected that the interfacial TiO_2 layer can be easily reduced. We will then demonstrate that the Schottky barrier height is strongly affected by oxygen deficiency. According to the present calculation, the interface is of Schottky-contact type for the fully oxidized interfacial TiO_2 while it becomes almost ohmic for strongly reduced one.

DOI: 10.1103/PhysRevB.80.195302 PACS number(s): 73.20.−r, 73.40.Rw, 71.15.Mb

I. INTRODUCTION

Reversible resistance-switching phenomena in transition-metal oxides such as NiO,[1] TiO_2,[2] and $SrTiO_3$ (Ref. 3) have attracted considerable attention for application to resistance-switching random access memory (ReRAM). Among these metal oxides, TiO_2 has been also expected as memristive switching material[4,5] and diode polarity switching material,[6] and the rectifying behavior of Pt/TiO_2/Pt structures is required for both switching mechanisms. A recent study[7] on the rectifying property of Pt/TiO_2/metal structures suggests that TiO_2 in contact with Pt top electrode (TE) may be well oxidized, causing the Schottky barrier at the TiO_2/Pt-TE interface, and that the interface between Pt bottom electrode and TiO_2 may be in an ohmic-contact state. Although it has been pointed out that the stoichiometry near interfaces affects the conductive property, the microscopic origin is not yet clear.

On the theoretical side, the density-functional theory (DFT) (Refs. 8 and 9) has become a widely used tool for calculations of properties of solids and molecules. A standard implementation of DFT is based on the Kohn-Sham equation and the use of the local-density approximation (LDA) (Ref. 10) or the generalized gradient approximation (GGA).[11] According to standard DFT calculations, the defect states of oxygen vacancy in TiO_2 are located in the conduction band and the excess electrons are delocalized over several Ti ions.[12,13] These results are in contradiction with the experiments; the introduction of oxygen vacancies creates defect states in the band gap ~0.8 eV below the conduction-band bottom[14,15] and these are assigned to Ti^{3+} 3*d* states by the electron-paramagnetic-resonance experiments.[16–18] The failure of the standard DFT calculation in describing the electronic structure of an oxygen vacancy in TiO_2 have been reviewed and discussed in recent publications.[19,20] Practical ways to correct some of these deficiencies are to use hybrid functionals or the so-called LDA/GGA+*U* approach.[21–24,26] As for metal/TiO_2 interfaces, some groups have investigated effects of metal species and stoichiometry at metal/rutile-TiO_2 interface within the standard LDA/GGA approach.[25–30] Since the discussion on the effect of stoichiometry requires the reasonable description of defect states, beyond LDA/GGA approach should be adopted.

TiO_2 crystallizes in the three different phases: rutile, anatase, and brokite. Rutile is the thermodynamically most stable bulk phase but anatase is technologically more important than rutile. Fujimoto *et al.*[31] demonstrated high-speed resistive change in a ReRAM memory cell with anatase nanolayer. In this paper, we investigate the electronic property of the Pt/anatase-TiO_2 interfaces with GGA+*U*. Particular attention has been paid to the dependence of Schottky barrier height (SBH) on the stoichiometry at the interface and the formation energy of oxygen vacancy.

II. COMPUTATIONAL DETAILS

The present calculations were performed by using our in-house computational code QMAS (Quantum MAterials Simulator).[32–34] We adopted the projector-augmented wave (PAW) method[35–37] with GGA (Ref. 11) for the electronic exchange and correlation interactions and GGA+*U* (Ref. 38) with the effective Hubbard-*U* parameter $U_{\mathrm{eff}}=U-J=5.0$ eV for Ti 3*d* orbitals. Note that U_{eff} is applied only within the augmentation region of PAW method. Therefore the present value of U_{eff} may correspond to a smaller value when U_{eff} is applied to the atomic sphere (see a comment as Ref. 20 in Ref. 39). The plane-wave energy cutoff was set to 20.0 hartree. The convergence criterion for maximum force amplitude was 1.0×10^{-4} hartree/bohr. The calculations of the layer-decomposed local density of states (LDOS) were performed using a real-space projection of the total density of states, and the calculations of the orbital-decomposed partial density of states (PDOS) were performed using a projection of the plane-wave states onto a localized linear combination of atomic-orbitals basis set.[40]

III. RESULTS

A. Bulk anatase

Structural parameters of bulk anatase TiO_2 optimized with GGA+*U* are $a=3.832$ Å, $c/a=2.528$, and $u=0.207$. These

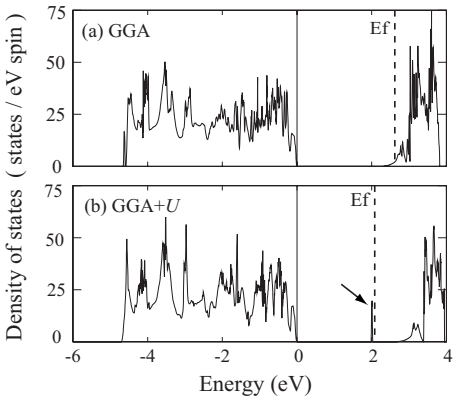

FIG. 1. Total density of states for the system with an oxygen vacancy with (a) GGA and (b) GGA+U with U_{eff}=5.0 eV. The top of the valence band is taken as the zero of energy. The Fermi energy is also shown. The arrow indicates the vacancy state.

are in good agreement with the experimental values:[41] a=3.782 Å, c/a=2.512, and u=0.208, and other theoretical one in LDA.[42] The introduction of the Hubbard U improves the energy gap from 2.20 eV with GGA to 2.65 eV, which is still smaller than the experimental value of 3.2 eV.[43]

B. Oxygen vacancy in bulk anatase

To understand the role of oxygen vacancy near interfaces, first, we adopted a simple picture of an oxygen vacancy in bulk anatase TiO_2. A 108-atom supercell made of $3\times3\times1$ unit cells was used. The oxygen vacancy was created simply by taking out one oxygen atom from the supercell. We found that the ground state is nonmagnetic even with spin-polarized GGA+U. Surrounding Ti atoms are displaced by 0.08–0.14 Å outward from the vacancy site. Atomic displacement with GGA+U is smaller than that with GGA (0.21–0.25 Å).

The removal of one oxygen atom introduces two excess electrons and there are two possible types of states: the excess electrons occupy delocalized conduction-band states which leads to a metallic ground state (with GGA) or localized states in the band gap (with GGA+U). The former case with GGA is shown in Fig. 1(a) while the latter case with GGA+U has the vacancy state located in the band gap, 0.69 eV below the conduction-band bottom [Fig. 1(b)]. Figure 2(a) shows the square of the wave function of the vacancy state with GGA+U. One can see the localization on the three Ti ions surrounding the oxygen vacancy. The partial density of states for one of the three Ti ions shows that the localized vacancy state mainly consists of Ti $d_{3z^2-r^2}$-type orbital with the local z axis along the vacancy-Ti direction [Fig. 2(b)].

The formation energy of an oxygen vacancy is calculated using the total energies of the supercell. In general, the formation energy for a neutral oxygen vacancy depends on an oxygen chemical potential as follows:

$$E_{\mathrm{form}}(V_{\mathrm{O}}) = E_{\mathrm{tot}}(V_{\mathrm{O}}) - E_{\mathrm{tot}}(\mathrm{perfect}) + \mu_{\mathrm{O}}, \qquad (1)$$

where E_{tot} (perfect) is the total energy of the nondefective supercell and $E_{\mathrm{tot}}(V_{\mathrm{O}})$ is the total energy of the supercell

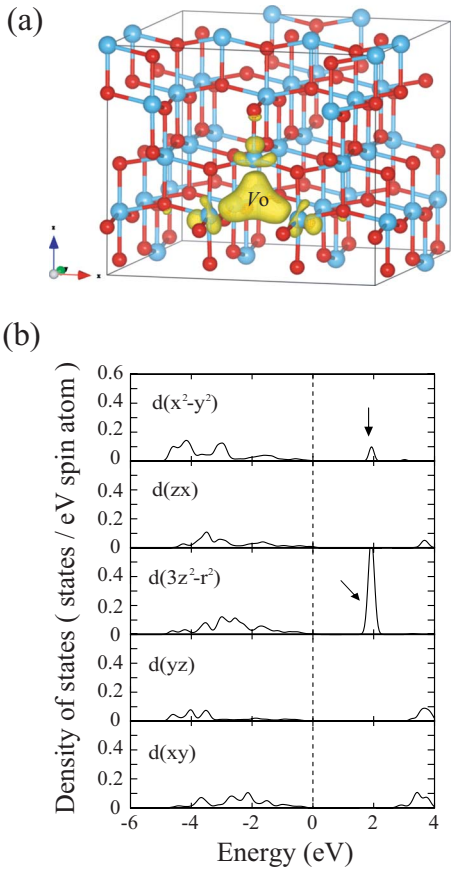

FIG. 2. (Color online) (a) The electron-density isosurface for the vacancy state with GGA+U. The isosurface of 0.008 electrons/a.u.^{3} is shown. (b) The PDOS for one of the three Ti atoms surrounding the oxygen vacancy is shown. The top of the valence band is taken as the zero of energy. The arrows indicate the vacancy state. A red (dark gray) ball denotes an O atom and blue one (light gray) a Ti atom.

containing a neutral oxygen vacancy. μ_{O} is an oxygen chemical potential. Assuming μ_{O} is half the total energy of an oxygen molecule in a triplet state, the formation energy of an oxygen vacancy is 4.34 eV with GGA and 5.25 eV with GGA+U. We did not use a correction for the O_2 overbinding suggested in Ref. 44.

Previously reported values, in which half of the total energy of an oxygen molecule is taken as μ_{O}, range from 4.2 to 5.3 eV, and the scattering in the calculated vacancy formation energy comes mainly from the use of different supercell size.[19]

C. Pt/TiO_2 interface

1. Interface system

In order to investigate the effect of stoichiometry at the interface on SBH, we have performed the GGA+U calculations on Pt/anatase-TiO_2 interfaces. In this study, we deal with a simple interface model of fcc-Pt(001)/anatase TiO_2(001). Figure 3 shows a unit cell of the model system which consists of four Pt layers epitaxially built on nine TiO_2 layers with the vacuum of 15 Å. The x and y dimensions of

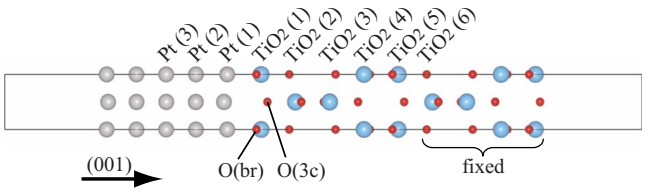

FIG. 3. (Color online) A schematic picture of the unit cell of the Pt/TiO_2 interface. The model system consists of five Pt layers epitaxially built on nine layers of TiO_2. When optimizing atomic positions, atoms in the outer five TiO_2 layers are fixed. A light gray ball denotes a Pt atom, small red one an O atom, and blue one (medium gray) a Ti atom.

the supercell are fixed at one of optimized lattice parameters of bulk anatase (3.832 Å). This reflects an experimental condition that a metal electrode is deposited on top of TiO_2. The theoretical lattice mismatch between Pt and anatase TiO_2 is 2.3%. The interfacial Pt atom is located on the on-top site above the bridging oxygen [O(br)] atom. It might be necessary to perform a series of calculations with different interfacial configurations. In real materials, atomic configurations near interfaces are very complicated and it would be impossible to really separate the effect of atomic configuration and stoichiometry. Furthermore, several TiO_x phases at Pt/TiO_2 interfaces have been obtained experimentally and theoretically.[45–47] The present study is a model calculation where we would like to see the effect of interfacial stoichiometry. For a reduced interface, oxygen atoms [O(br) and O(3*c*)] in the interfacial $TiO_2(1)$ layer are taken out, which corresponds to $Pt/Ti/TiO_2$ system. When optimizing the atomic positions, atoms in four TiO_2 layers are fixed as shown in Fig. 3.

2. Stoichiometric interface

The bond length between interfacial Pt and O atoms is 2.08 Å, which is slightly longer than 1.93 Å in the system of one monolayer adsorption of Pt on the stoichiometric rutile-TiO_2(110) surface.[28]

Figure 4 shows the LDOS for each Pt and TiO_2 layer. The Fermi level is taken as the zero of energy. At the interface, clear evidence of strong O *p*-Pt *d* hybridization can be seen in the LDOS of Pt(1) and $TiO_2(1)$, see also the partial density of states (PDOS) in Fig. 5 for *d* state of Pt(1) and *p* state of the bridging O [O(br)]. The center of gravity of Pt(1) LDOS is shifted upward in energy and that of the *p*-band part of $TiO_2(1)$ LDOS downward. The LDOS of the TiO_2 (6) layer, near the middle of TiO_2 slab, is very similar to the DOS of the bulk anatase. The Fermi level is lying in the middle of a band gap. This interface is characterized as a Schottky contact with the conduction-band offset from the Fermi energy being 0.80 eV. In the LDOS of the interfacial TiO_2 (1) layer, one can observe the continuous spectrum of states in the band gap corresponding to the so-called MIGS (metal-induced gap states). To understand more details of the character of MIGS, we examined PDOS for Pt, Ti, and O atoms near the interface (Fig. 5). It is evident that O(br) contributes dominantly to MIGS, another consequence of hybridization between Pt *d* and O(br) *p* orbitals. The PDOS for

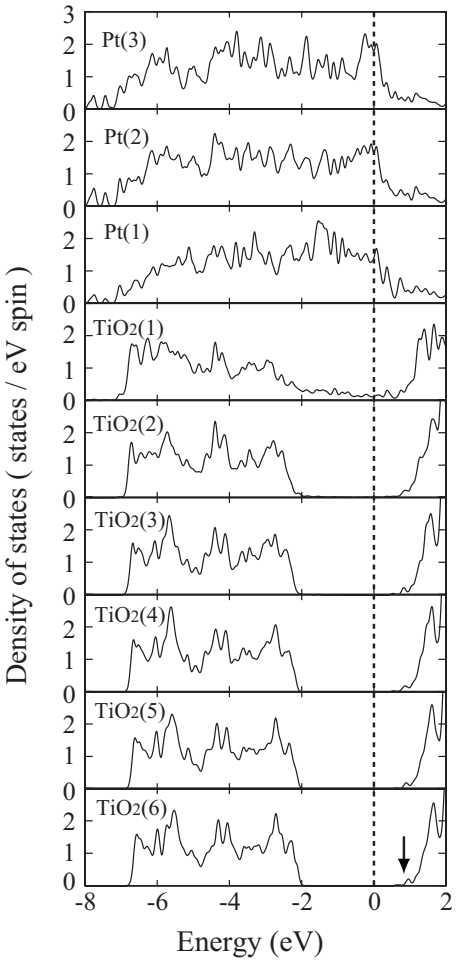

FIG. 4. The LDOS for each Pt and TiO_2 layer for the stoichiometric Pt/TiO_2 interface. The labels for layers are the same as in Fig. 3. The Fermi level is chosen as zero energy. The arrow indicates the conduction-band bottom in $TiO_2(6)$ layer as a guide to the eyes.

O(3*c*) has very small weight of MIGS and has a shape close to the bulk one. The partially occupied MIGS at the Fermi energy are expected to accommodate excess electrons introduced by the removal of oxygen atoms, which would make reduction easier at the interface.[48] This will be discussed further in Sec. III C 3.

3. Oxygen-vacancy formation near interface

As mentioned above, the interface would be more easily reduced than the bulk region due to the existence of MIGS. In order to confirm this, we calculated the formation energy of an oxygen vacancy as a function of the distance from the interface (Fig. 6). An oxygen vacancy is introduced by removing one oxygen atom from a 2×2 lateral (*xy*) supercell. The smaller the value is, the easier it is to create an oxygen vacancy. It is found that the formation energy is the lowest in the $TiO_2(1)$ layer. The formation energy saturates within the three TiO_2 layers to the value similar to the bulk-anatase value of 5.25 eV. The formation energy in $TiO_2(1)$ layer is smaller than that in the bulk by 2.33 eV. With GGA, the formation energy in $TiO_2(1)$ layer is 2.36 eV, which is

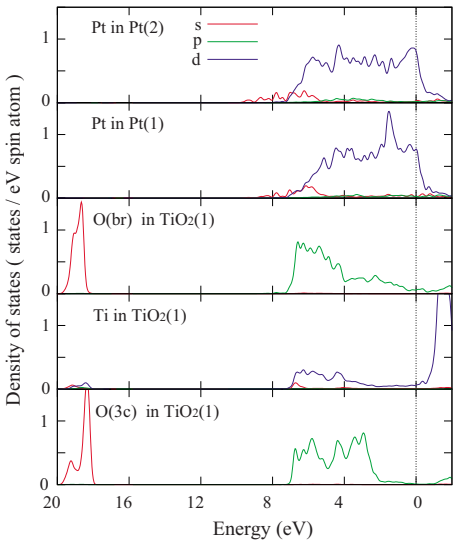

FIG. 5. (Color online) The PDOS for Pt, Ti, and O atoms for the stoichiometric Pt/TiO_2 interface. The labels for layers are the same as in Fig. 3. The Fermi level is chosen as zero energy.

smaller than that in the bulk by 1.98 eV. We have obtained a nonmagnetic solution for an oxygen vacancy in the bulk anatase with GGA+U as described in Sec. III B. On the other hand, as recently shown in Ref. 22, there are several solutions close in energy for this vacancy and the solutions may depend on the method used. However, as the variation in the oxygen-vacancy formation energy among these solutions is smaller than 0.6 eV, the present result that the formation energy is the lowest at the interface does not depend on the method used in the calculation.

Figure 7 shows the LDOS for each layer calculated with GGA+U for the system with an oxygen vacancy in the TiO_2(1) layer and the TiO_2(3) layer. When the oxygen vacancy is away from the interface, the vacancy state appears in the band gap [Fig. 7(b)] similarly to the case of an oxygen vacancy in the bulk [see Fig. 1(b)]. Note that this gap state could not be reproduced with GGA. Since the excess electrons introduced by the removal of an oxygen atom localize on the three Ti atoms surrounding the oxygen vacancy as shown in Fig. 2, a small structure related to the vacancy state can be observed in the LDOS of the TiO_2 (2) layer. On the other hand, no vacancy state is found in Fig. 7(a) since the excess electrons introduced by the removal of an oxygen atom are accommodated in the MIGS. This results in the lower formation energy at the interface. The fact that the cost

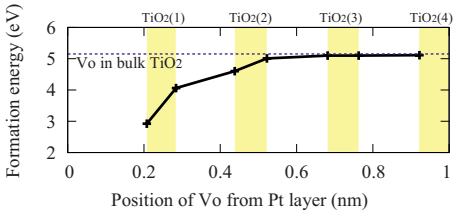

FIG. 6. (Color online) Formation energies of an oxygen vacancy as a function of the distance from Pt layer. The formation energy in the bulk anatase is also shown.

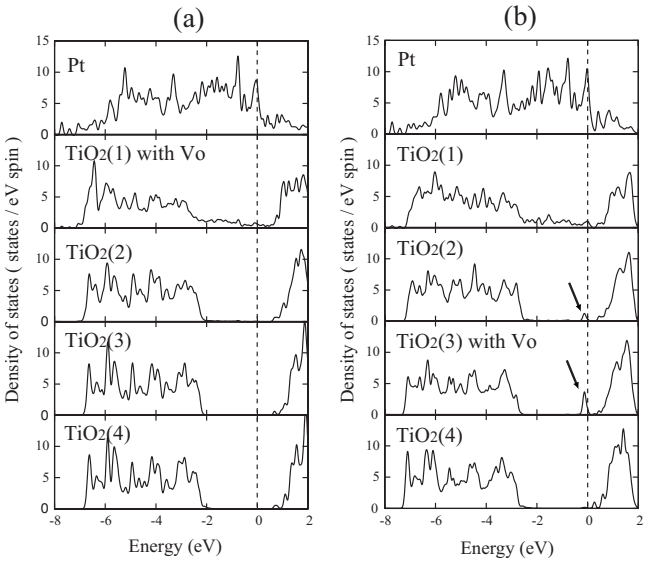

FIG. 7. The LDOS for each Pt and TiO_2 layer for the system with an oxygen vacancy in (a) TiO_2 (1) layer and (b) TiO_2 (3) layer. The Fermi level is chosen as zero energy. The arrows indicate the vacancy state.

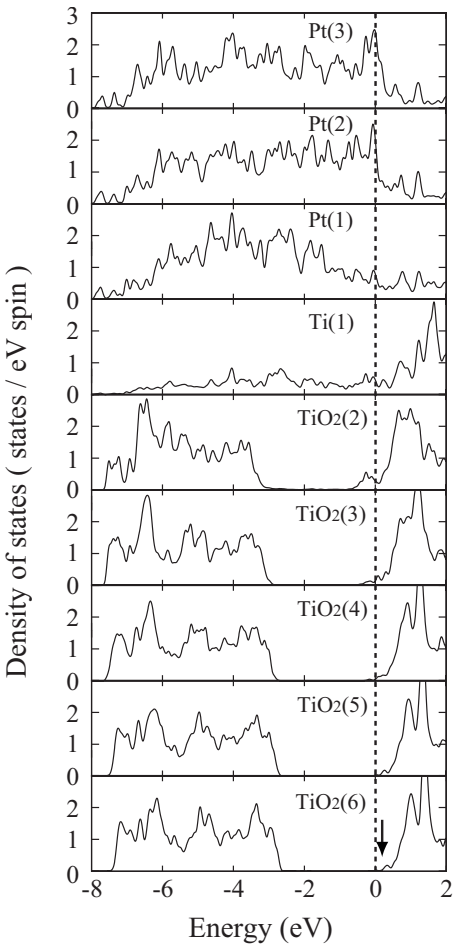

FIG. 8. The LDOS for each Pt and TiO_2 layer for the reduced Pt/TiO_2 interface. The labels for layers are the same as in Fig. 3. The Fermi level is chosen as zero energy. The arrow indicates the conduction-band bottom in TiO_2(6) layer as a guide to the eyes.

to creating an oxygen vacancy is lower at the interface than in the bulk has been found also for other metal/oxide interfaces, such as CeO_2,[48] MgO,[49–51] and HfO_2 (Refs. 52 and 53) systems.

4. Reduced interface

In order to study the electronic structure of highly reduced interface, all oxygen atoms in the interfacial TiO_2 (1) layer were removed. Figure 8 shows the LDOS for each of Pt and TiO_2 layers and the interface Ti layer. The LDOS of Ti(1) layer seems to be characterized as simply the tail of Pt(1). The LDOS of the TiO_2 (6) layer is very similar to the DOS of the bulk anatase as is for the stoichiometric interface. The Fermi level, however, is lying just bellow the bottom of the conduction band, indicating that this interface is almost an ohmic contact. Because of the absence of interface oxygen, there is no Pt *d*-O(br)*p* hybridization and the center of gravity of Pt(1) *d* band comes down in energy.

IV. CONCLUSION

We have shown that the formation of the stoichiometric Pt/TiO_2 interface induces the MIGS in the band gap of TiO_2. These states have appreciable weight in the interface layer only and decay strongly into the subinterface layer. In the bulklike region of the TiO_2 slab, the Fermi level lies in the middle of band gap, which indicates that the stoichiometric interface is of a Schottky-contact type. We have demonstrated that the presence of MIGS reduces the formation energy of oxygen vacancy near the interface and therefore the interface can be easily reduced. One of the important consequences of the reduction in the interface TiO_2 layer is that the Fermi level shifts up to the bottom of the conduction band to make SBH smaller. These results are in good agreement with experimental findings of rectifying properties of $Pt/TiO_2/Pt$ structure. The present analysis provides a strong theoretical support to the experimental finding that the oxygen deficiency near interfaces plays a key role in the rectifying properties.

ACKNOWLEDGMENTS

We would like to thank M. Kohyama and S. Tanaka for helpful discussions on recent theoretical studies of metal/oxides interfaces. We also would like to thank H. Akinaga, H. Shima, N. Zhong, H. Akoh, A. Sawa, I. H. Inoue, H. Sato, and P. Xiang for discussions. This work is partly supported by the Next Generation Supercomputing Project, Nanoscience Program.

[1] S. Seo, M. J. Lee, D. H. Seo, E. J. Jeoung, D.-S. Suh, Y. S. Joung, I. K. Yoo, I. R. Hwang, S. H. Kim, I. S. Byun, J.-S. Kim, J. S. Choi, and B. H. Park, Appl. Phys. Lett. **85**, 5655 (2004).
[2] C. Rohde, B. J. Choi, D. S. Jeong, S. Choi, J. S. Zhao, and C. S. Hwang, Appl. Phys. Lett. **86**, 262907 (2005).
[3] Y. Watanabe, J. G. Bednorz, A. Bietsch, Ch. Gerber, D. Widmer, A. Beck, and S. J. Wind, Appl. Phys. Lett. **78**, 3738 (2001).
[4] D. B. Strukov, G. S. Snider, D. R. Stewart, and R. S. Williams, Nature (London) **453**, 80 (2008).
[5] J. J. Yang, M. D. Pickett, X. Li, D. A. A. Ohlberg, D. R. Stewart, and R. S. Williams, Nat. Nanotechnol. **3**, 429 (2008).
[6] J. R. Jameson, Y. Fukuzumi, Z. Wang, P. Griffin, K. Tsunoda, G. I. Meijer, and Y. Nishii, Appl. Phys. Lett. **91**, 112101 (2007).
[7] H. Shima, F. Takano, H. Muramatsu, H. Akinaga, I. H. Inoue, and H. Takagi, Appl. Phys. Lett. **92**, 043510 (2008).
[8] P. Hohenberg and W. Kohn, Phys. Rev. **136**, B864 (1964).
[9] W. Kohn and L. J. Sham, Phys. Rev. **140**, A1133 (1965).
[10] J. P. Perdew and A. Zunger, Phys. Rev. B **23**, 5048 (1981).
[11] J. P. Perdew, K. Burke, and M. Ernzerhof, Phys. Rev. Lett. **77**, 3865 (1996).
[12] E. Cho, S. Han, H.-S. Ahn, K.-R. Lee, S.-K. Kim, and C.-S. Hwang, Phys. Rev. B **73**, 193202 (2006).
[13] S. Na-Phattalung, M. F. Smith, K. Kim, M.-H. Du, S.-H. Wei, S. B. Zhang, and S. Limpijumnong, Phys. Rev. B **73**, 125205 (2006).
[14] M. A. Henderson, W. S. Epling, C. H. F. Peden, and C. L. Perkins, J. Phys. Chem. B **107**, 534 (2003).
[15] R. L. Kurtz, R. Stockbauer, T. E. Medey, E. Roman, and J. L. De Segovia, Surf. Sci. **218**, 178 (1989).
[16] E. Serwicka, M. W. Schlierkamp, and R. N. Schindler, Z. Naturforsch. A **36A**, 226 (1981).
[17] T. Berger, M. Sterrer, O. Diwald, E. Knözinger, D. Panayotov, T. L. Thompson, and J. T. Yates, J. Phys. Chem. B **109**, 6061 (2005).
[18] D. C. Hurum, A. G. Agrios, K. A. Gray, T. Rajh, and M. C. Thurnauer, J. Phys. Chem. B **107**, 4545 (2003).
[19] M. V. Ganduglia-Pirovano, A. Hofmann, and J. Sauer, Surf. Sci. Rep. **62**, 219 (2007).
[20] G. Pacchioni, J. Chem. Phys. **128**, 182505 (2008).
[21] C. Di Valentin, G. Pacchioni, and A. Selloni, Phys. Rev. Lett. **97**, 166803 (2006).
[22] E. Finazzi, C. Di Valentin, G. Pacchioni, and A. Selloni, J. Chem. Phys. **129**, 154113 (2008).
[23] B. J. Morgan and G. W. Watson, Surf. Sci. **601**, 5034 (2007).
[24] G. Mattioli, F. Filippone, P. Alippi, and A. Amore Bonapasta, Phys. Rev. B **78**, 241201(R) (2008).
[25] L. Thien-Nga and A. T. Paxton, Phys. Rev. B **58**, 13233 (1998).
[26] Z. Yang, R. Wu, and D. W. Goodman, Phys. Rev. B **61**, 14066 (2000).
[27] K. Okazaki, Y. Morikawa, S. Tanaka, K. Tanaka, and M. Kohyama, Phys. Rev. B **69**, 235404 (2004).
[28] K. Okazaki, Y. Morikawa, S. Tanaka, K. Tanaka, and M. Kohyama, J. Mater. Sci. **40**, 3075 (2005).
[29] K. Okazaki-Maeda, Y. Morikawa, S. Ichikawa, S. Tanaka, and M. Kohyama, Mater. Trans. **47**, 2669 (2006).
[30] I. Marri and S. Ossicini, Solid State Commun. **147**, 205 (2008).
[31] M. Fujimoto, H. Koyama, M. Konagai, Y. Hosoi, K. Ishihara, S. Ohnishi, and N. Awaya, Appl. Phys. Lett. **89**, 223509 (2006).
[32] S. Ishibashi, T. Tamura, S. Tanaka, M. Kohyama, and K. Terakura, Phys. Rev. B **76**, 153310 (2007).

[33] S. Ishibashi, K. Terakura, and H. Hosono, J. Phys. Soc. Jpn. **77**, 053709 (2008).
[34] T. Tamura, S. Ishibashi, S. Tanaka, M. Kohyama, and M.-H. Lee, Phys. Rev. B **77**, 085207 (2008).
[35] P. E. Blöchl, Phys. Rev. B **50**, 17953 (1994).
[36] N. A. W. Holzwarth, G. E. Matthews, R. B. Dunning, A. R. Tackett, and Y. Zeng, Phys. Rev. B **55**, 2005 (1997).
[37] G. Kresse and D. Joubert, Phys. Rev. B **59**, 1758 (1999).
[38] V. I. Anisimov, J. Zaanen, and O. K. Andersen, Phys. Rev. B **44**, 943 (1991).
[39] H. Weng, T. Ozaki, and K. Terakura, J. Phys. Soc. Jpn. **77**, 014301 (2008).
[40] D. Sanchez-Portal, E. Artacho, and J. M. Soler, Solid State Commun. **95**, 685 (1995).
[41] J. K. Burdett, T. Hughbanks, G. J. Miller, J. W. Richardson, Jr., and J. V. Smith, J. Am. Chem. Soc. **109**, 3639 (1987).
[42] R. Asahi, Y. Taga, W. Mannstadt, and A. J. Freeman, Phys. Rev. B **61**, 7459 (2000).
[43] H. Tang, H. Berger, P. E. Schmid, F. Lévy, and G. Burri, Solid State Commun. **87**, 847 (1993).
[44] L. Wang, T. Maxisch, and G. Ceder, Phys. Rev. B **73**, 195107 (2006).
[45] T. Orzali, M. Casarin, G. Granozzi, M. Sambi, and A. Vittadini, Phys. Rev. Lett. **97**, 156101 (2006).
[46] F. Sedona, G. Granozzi, G. Barcaro, and A. Fortunelli, Phys. Rev. B **77**, 115417 (2008).
[47] S. Agnoli, T. Onur Mentes, M. A. Nino, A. Locatelli, and G. Granozzi, Phys. Chem. Chem. Phys. **11**, 3727 (2009).
[48] Z. Yang, Z. Lu, G. Luo, and K. Hermansson, Phys. Lett. A **369**, 132 (2007).
[49] D. M. Duffy, J. H. Harding, and A. M. Stoneham, J. Appl. Phys. **76**, 2791 (1994).
[50] L. Giordano, J. Goniakowski, and G. Pacchioni, Phys. Rev. B **64**, 075417 (2001).
[51] J. Carrasco, N. Lopez, F. Illas, and H.-J. Freund, J. Chem. Phys. **125**, 074711 (2006).
[52] C. Tang and R. Ramparasad, Appl. Phys. Lett. **92**, 182908 (2008).
[53] E. Cho, B. Lee, C. Lee, S. Han, S. Jeon, B. Park, and Y. Kim, Appl. Phys. Lett. **92**, 233118 (2008).